Supporting Information

Mayo and Sommer 10.1073/pnas.1217177110

SI Methods

Subjects and Neuronal Recordings. Subjects were two adult male rhesus monkeys (*Macaca mulatta*, 7 and 9 kg). Data-collection procedures were identical to those previously detailed (1). Briefly, the frontal eye field (FEF) and superior colliculus (SC) were identified based on a combination of stereotaxic location, structural MRI, microstimulation, and established physiological properties (2–4). The superficial layers of the SC were defined as the initial 1 mm of transient visual responses upon first entering the SC. For acceptance into our dataset, neurons in the intermediate layers of the SC had to be at least 1-mm below the top of the SC (average 1–3 mm). Intermediate SC neurons were generally recorded only after encountering other neurons that showed saccade-related activity. In all three areas, neurons were selected for recording only if they were visually responsive in the receptive-field (RF) mapping task. Eccentricities of RF centers across the neuronal populations were 14.7 ± 9.0, 11.2 ± 13, and 12.1 ± 10.7° for FEF, visuomotor intermediate layers of the SC (intSC), and visual superficial layers of the SC (supSC), respectively (mean ± SEM). The FEF and SC are anatomically linked via a single synapse in the thalamus (5, 6), among other pathways. Although intSC and supSC are functionally distinct regions of the SC, they are different layers of the same brain structure (7). For expository purposes, we refer to them as different brain areas.

We recorded from 90 neurons in the FEF, 47 neurons in intSC, and 9 single neurons and 43 multiunit groups in supSC (monkey K: 41, 31, 9 neurons and 21 groups; monkey C: 49, 16, 22, respectively). Because single-unit and multiunit recordings from the supSC displayed similar patterns of activity, the data were pooled ($n = 52$).

Behavioral Task and Visual Stimuli. Monkeys sat in a primate chair with head restrained and facing a screen onto which visual stimuli were projected by an LCD projector. To start each trial, the monkey fixated a spot (0.3° square, 6 cd/m^2) in the center of the screen (fixation window: 1.5–2.2°). After ∼750 ms, the fixation point was turned off and a saccade target (0.3° square) appeared 12° to the right (contralateral to the recording hemisphere). This first saccade was used to control for motor activity that would otherwise be, in effect, random because of initial target acquisition during free viewing in the intertrial interval. After the saccade, the monkey maintained fixation (1.8–2.5° window) for 500–1,300 ms before two identical stimuli (50 ms each, 294 cd/m^2) were flashed consecutively in the RF center. We manipulated the amount of time between the onsets of the two stimuli (stimulus onset asynchrony, SOA) on each trial. Intervals were defined by the amount of time between two flashes (as opposed to the duration of a single flash) to facilitate the measurement of changes in neuronal activity because response onsets can be measured more precisely than response offsets. SOAs ranged from 250 to 450 ms at ∼16.7 ms intervals (frame rate of 60 Hz projector). Stimulus size was scaled with RF eccentricity (8). After the two stimuli were flashed, a second delay period (200–1,000 ms) occurred. After the delay, two choice targets appeared in the visual field ipsilateral to the recording hemisphere; one target 6° above, the other 6° below the initial fixation point (now extinguished).

Monkeys indicated whether the time interval's SOA was shorter or longer than a learned reference interval of 350 ms by making a saccade to one of the two choice targets. For monkey K, "short" choices were indicated by a saccade to the upper green choice target and "long" choices were indicated by saccades to the lower red choice target. The response mapping was reversed for monkey C (upper red "long" target and lower green "short" target). Choice targets were photometrically isoluminant (40 cd/m^2; Photo Research, model PR-655). Saccade target locations were fixed within a block of trials. If the initial rightward saccade target was close to the RF center, the saccade target and relative choice target locations were rotated 45° away from the RF, so that the initial saccade was either up-right or down-right. Thus, the initial saccade was always at least 45° away from the RF center. Correct judgments were reinforced with a liquid reward and incorrect judgments and aborted trials resulted in a brief timeout and no reward.

During a given recording session, we presented five or six time intervals ("test intervals" for that session) pseudorandomly interleaved for each neuron. Test intervals were chosen on a daily basis to obtain a range of behavioral performance. The set of test intervals during a session was always symmetrical around the reference interval. For example, whenever an SOA of 300 ms was used (a short trial 50 ms less than the reference interval), the complementary long SOA of 400 ms (50 ms greater than the reference interval) was also used. When the reference interval itself was presented as a test interval, only five total intervals were used: two short intervals, two long intervals, and the reference interval. Reference interval trials were excluded from all analyses except where noted. There were small (<2 ms), highly significant differences in reaction time for each monkey as a function of trial success (rank-sum test, monkey K: correct > incorrect, $P < 10^{-3}$; monkey C: incorrect > correct, $P < 10^{-3}$).

Neuronal Activity and Response Epochs. Visual activity was measured during visual epochs, 50–150, 30–130, and 20–70 ms after stimulus onset, for the FEF, intSC, and supSC, respectively. These epochs were selected to match the observed onsets and durations of visual responses in each area. For all areas, saccade-related activity was measured −50 to 0 ms around saccade onset and delay activity was measured 100 ms before the second stimulus onset, during the interstimulus interval. Baseline activity was measured 100 ms before first stimulus onset. All response epochs were verified using averaged population responses. "Visually responsive" neurons were those that showed significantly greater activity during the visual response epochs compared with the baseline epoch for two or more time intervals (t test, $P < 0.05$).

A minimum of four trials was required for inclusion in a particular condition's dataset (e.g., correct/incorrect trials at a particular time interval). Increasing this minimum up to 10 trials did not alter our main results but resulted in less statistical power at extreme time intervals where fewer incorrect trials occurred. We found no major differences between recording locations within an area or between animals and therefore combined data for neuronal analyses. We used a Gaussian kernel with 10-ms SD to create all spike-density functions (9). We also used a 5-ms SD kernel for latency analyses (see below).

We collected an average of 35 correct trials per SOA (range: 6–69). We collected an average of 268 completed trials per neuron, yielding 28,100 total trials from monkey K and 22,618 total trials from monkey C. Correlations, coefficients of determination (r^2), and associated P values were calculated using the corrcoef function in MATLAB (Mathworks). Nonparametric statistical tests were used whenever we could not ensure that the data were normally distributed. Wilcoxon signed-rank tests were used to assess changes in response strength and interresponse timing between correct and incorrect trials (Fig. 3, Fig. S1, and

Tables S3 and S4). Comparable unpaired tests produced similar results. Permutation tests were used to assess the significance of choice probability data (Fig. 5). Other statistical tests are noted in text. Statistical significance was defined as $P < 0.05$. P values less than 0.001 are denoted as $< 10^{-3}$.

Population Responses. Difference signals were created by subtracting incorrect from correct population spike-density functions for each time interval and averaging the resulting activity (Fig. 4*B* and Fig. S2). Before combining for population measures, individual neurons were normalized to their peak visual response to the first visual stimulus across all trials. We tested for a significant difference between short- and long-difference signals using a permutation test. At each analysis window timepoint (window width, 100 ms; step size, 20 ms) starting at first stimulus onset, we measured the difference in firing rate between the means of the two difference signal populations.

Latency. We calculated visual response latencies by separately using spike density functions (SDFs) and raw spike counts. Our main two methods relied on analysis of the SDFs. We compiled the trials from each condition (e.g., correct/incorrect trials at a particular time interval) and created the neuron's SDF for that condition's activity. The first latency metric defined visual response onset as the point in time, relative to stimulus onset, in which the SDF increased two SDs above the baseline activity level for more than 5 ms (SD2). An analogous measurement was used to determine response offset except that we measured the time after the response's peak firing rate in which the activity declined to within two SDs above the baseline firing rate, relative to stimulus offset.

The second latency metric (Peak) defined visual response onset as the time required for the response to reach its maximum firing rate during the visual epoch, relative to stimulus onset. SD2 and Peak latency values were calculated for each of the two visual responses in every condition. Latency measurements were verified by visual inspection and spurious latencies were discarded.

An additional measure of response latency, MaxDiff, defined the response latency as the time at which the visual response and baseline activity maximally differed (10). This measure involved sliding an analysis window, of variable sizes up to the size of the visual epoch, over the entire visual response. Spike counts in this response window were iteratively compared (via t test) to those in an equivalent window during the baseline activity. Results from this spike-based latency measure were consistent with our SDF latency measures (Table S1). Correlations between methods were strong and highly significant in all areas ($P < 10^{-3}$). We therefore relied exclusively on the computationally less-demanding SD2 and Peak methods.

We also used a bootstrap method on the peak latency values of both first and second visual responses for all neurons. We used the Peak metric for bootstrapping because it was more likely to provide an unambiguous time point for neurons in the dataset. For each condition for each neuron, we randomly sampled with replacement the original number of trials. We calculated the latency of the visual response for each resampled set of spike times. We repeated this procedure 1,000 times to obtain a distribution, which estimated the variation of the mean latency values given the original spike times. The SD of this distribution was then used as a measure of the standard error (SE) of the original latency value (11, 12).

Choice Probability. We used receiver operating characteristic (ROC) methods to measure the discriminability of distributions of firing rates by an ideal observer (13, 14). To facilitate comparisons between brain regions and span the time during which the animal was required to make a judgment, we sampled 1,000 ms of neuronal activity following first-stimulus onset to include the two visual responses and early delay activity on all trials. (Mean time from first-stimulus onset to choice-saccade onset was 1,071 ms.) For each neuron, we normalized activity at each time interval by subtracting the neuron's average baseline activity and dividing by its SD (z-correction). This correction minimized bias effects caused by individual neurons with exceptionally high firing rates or highly variable responses. We arranged all ROC statistics such that if the area under the ROC curve (AUC) was greater than 0.5, then long choice trials contained higher firing rates. We calculated the AUC for each time interval for each neuron. Choice probability (CP) was then defined as the AUC (Fig. 5*A*). Mean CP values limited to the second visual epoch only were greater than 0.5 at all intervals in the FEF (12 of 12, 100%), compared with only 50% and 42% in the intSC and supSC, respectively. Grand choice probability (gCP) (Fig. 5 *B–D*) (15) was calculated by determining the AUC for the distributions of firing rates across all trials for a given neuron, sorted according to short or long choices. gCP was defined as the AUC across time intervals for each neuron. For reference, the representative FEF neurons in Fig. 2 had gCPs of 0.67, 0.68, and 0.59, respectively. Statistical significance of CP distributions, differences between them, and grand CP values per neuron were evaluated using permutation tests.

Microsaccades. Following previous work (16, 17), microsaccades had to meet the following criteria: eye position velocity greater than 8°/s, surpass an acceleration threshold of 650°/s^2, and last for longer than 8 ms (18). Because we were primarily interested in changes in neuronal activity close to when the time intervals were presented, we measured microsaccades during the fixation period after the first saccade offset until just before the saccade to one of the choice targets.

SI Results

Interaction Between Latency and Strength of Visual Responses. There was the potential to find a latency effect attributable to related changes in strength (19). Our Peak metric was therefore particularly useful because it was not prone to finding latencies that depended on changes in the strength of visual responses, unlike other latency measures based on statistical criteria. Accordingly, a correlation between the latency and strength of first visual responses in the FEF reached significant levels using the SD2 method (using SDF = 10 ms; P value of correlation coefficient = 0.04), but was not significant for the Peak method (using SDF = 10 ms; $P = 0.70$). To be conservative, we considered strength and latency changes separately.

General Properties of Visual Response Latencies. Our basic FEF latency results (Table S1) were similar to previous detailed work on FEF response latencies (20). This group used four other latency methods, most based on Poisson spike train analysis, and found few differences between their four methods. The fact that our population results fit with their results, as well as with classic reports of FEF latencies (21), suggests that latency measures are robust across laboratories and largely independent of the specific latency metric used.

The latency hypothesis required that we measure the amount of time between visual responses. To do so, we calculated the latency of first and second visual responses separately (Table S2). We found that second visual responses were accelerated in all brain areas tested relative to first visual responses; second responses started, peaked, and ended sooner than their first-response counterparts. This result is likely because in some cases the initiation of second responses occurred but residual activity related to the first visual responses had not fully decayed. However, the difference between first and second responses was not simply a shift in response time relative to stimulus onset. Second visual responses were shorter in duration than first visual responses as

well (Table S2, rightmost column). This effect was highly significant in all brain areas tested (signed-rank test, $P < 10^{-3}$).

Our preliminary analyses confirmed that visual response latencies in our task were consistent with results from other tasks and laboratories. We therefore turned our attention to measuring the time between first and second visual responses in each trial to see if it encoded the monkey's perceptual report of time interval.

In light of our clear positive results related to the strength hypothesis (e.g., Fig. 3*C*), we considered our negative results related to the latency hypothesis to be critical, and so we summarize them using tables. Table S3 shows the FEF latency dataset and Table S4 shows the latency data for both the intSC and supSC. The tables contain the information regarding differences in correct versus incorrect interresponse timings. The data include mean interresponse time for correct and incorrect trials and the correlation coefficient. P values were $< 10^{-3}$ for all correlations (Tables S3 and S4). Because the latency hypothesis makes contrasting predictions for short and long time intervals, data were subdivided by interval group (columns). Statistical significance of the difference between correct and incorrect responses is indicated by the color of each cell. Red shading indicates significance as predicted by the latency hypothesis. Gray shading indicates significance in the direction opposite to that predicted by the latency hypothesis. If the latency hypothesis is true, then we expect to see two red boxes, horizontally side-by-side in the same row (for both short and long intervals). We specifically designed this analysis to be as analogous to the strength analysis as possible.

Time between response onsets. We first analyzed the amount of time between visual response onsets (response onset asynchrony; ROA) using the SD2 metric (Tables S3, row A and S4, rows A and F). In the FEF and intSC we found no significant changes in response latency that fit with the latency hypothesis. In fact, the only significant result for the FEF contradicted the hypothesis (Table S3, row A). We found that ROAs in the FEF were significantly longer in incorrect long trials than in correct long trials ($P = 0.04$). In this case, monkeys chose the short choice target even though the amount of time between visual responses increased relative to correct long responses. In the supSC, ROAs were significantly elongated for short time intervals in support of the latency hypothesis ($P < 10^{-3}$). There was no evidence of a corresponding change in the responses to long time intervals (Table S4, row F).

We found no significant results when using the Peak latency metric on the same data (Tables S3, row B and S4, rows B and G). Peak responses naturally occurred later than the onset time to two SDs above baseline activity. In principle, it is possible that the few significant differences found in the FEF and supSC using the SD2 metric were lost later when neuronal responses reached their peak firing rates. However, unlike the complementary changes found for visual response strengths in both short and long SOA trials, we found no complementary changes in the time between visual response onsets.

Other measures of interresponse time. Our task did not require the monkeys to use stimulus onsets to measure the intervening time between stimuli, nor can we be certain a priori that the brain relies on the time between visual response onsets. In principle, any combination of onsets and offsets could be used as reference points to measure the presented time intervals: onset-onset, onset-offset, offset-onset, and offset-offset. Although referencing the two stimulus onsets (and corresponding neuronal response onsets) is arguably the most natural approach, for thoroughness we tested whether latency information was embedded in other response combinations. We repeated the interresponse timing analysis process for all remaining possibilities (onset-offset, offset-onset, and offset-offset), using both SD2 and Peak metrics for detecting onset. The amount of time between first-response onset and second-response offset using the SD2 metric is shown in Tables S3, row C and S4, rows C and H. For this metric, as in all remaining interresponse timing possibilities, we failed to find a complementary change in which short and long time intervals showed significant changes in opposing directions, which would be consistent with latency encoding of time intervals.

Bootstrapped latency values. We tested whether the more reliable neurons in our populations might provide more useful timing information regarding the monkeys' choices. We did this in two ways. First, we replaced each neuron's original latencies with the means of the resampled latency distributions of each condition (*Methods*). Given random shuffling of each condition's original trials, the mean of the resampled distribution may be considered a more reliable measure of the neuron's response latency. After using the Peak metric to measure ROAs, we plotted correct versus incorrect resampled ROAs for short and long trials (Tables S3, row D and S4, rows D and I). Compared with the original latency data (Tables S3, row B and S4, rows B and G), mean resampled latencies accounted for more of the variance. However, we found no significant differences using ROAs calculated from the original latencies. Here, we found a single significant difference in ROAs, between correct and incorrect ROAs, in long trials. This difference was not significant for the same data convolved with a smaller Gaussian kernel. This analysis therefore provided limited evidence to support the latency hypothesis, but it was not robust and failed to account for behavioral performance in short time intervals.

Second, we also performed the same analysis using only our most reliable neurons, as measured by the SD of the neurons' resampled latency distributions (*Methods*). For each area, we looked at the half of our neurons (the top 50%) with the most reliable visual response onsets (Tables S3, row E and S4, rows E and J). Our results mirrored what we found when using the mean of the shuffled distributions. FEF ROAs were significantly longer in correct long trials compared with those of incorrect long trials, as predicted by the latency hypothesis. However, again we did not see a significant difference in short trials in any of the three brain areas.

Sensitivity of interresponse timing analyses. To confirm that our analysis method was sensitive enough to detect potential latency changes, we compared correct population ROAs from two adjoining time intervals instead of our usual correct vs. incorrect comparison within the same time interval. In principle, these two populations should differ by ~17 ms, which is also approximately the amount of time visual responses might differ if the monkey incorrectly mistook one interval for another. Tests of adjoining correct ROAs (e.g., 317 and 333 ms) were highly significant (signed-rank test, $P < 10^{-3}$), indicating that our lack of support for the latency hypothesis was not simply because of a lack of statistical power.

Finally, we looked exclusively at the time intervals surrounding the reference interval (SOAs of 333 and 367 ms). We reasoned that the latency variations at these difficult time intervals were most likely to elicit incorrect choices because relatively small latency changes could "push" the interval closer or to the opposite side of the reference interval. However, even after looking at these time intervals in isolation, we found no significant change in the amount of time between visual responses as a function of task performance (e.g., onset-onset using SD2 metric and SDF = 10 ms, signed-rank test, SOA 333: $P = 0.53$, SOA 367 $P = 0.88$).

Influence of Premotor Activity on Changes in Response Strength. Because our main result pertains to significant strength changes in the FEF, we limit our discussion to that region. When neuronal isolation allowed, we recorded FEF responses during two additional tasks. First, we recorded neuronal responses ($n = 16$) outside of the time-discrimination task but with the same fixation and saccade locations in a delayed visually guided saccade task.

If strength changes were simply a result of changes in activity based on the saccade, our results could be explained by greater firing rates for saccades to the long-choice target location. We found that only two (12.5%) FEF neurons showed such a differential effect (rank-sum test, $P < 0.05$), well below the 44% of FEF neurons that showed significant activity in our time-interval discrimination task.

We also recorded from a subset of FEF neurons ($n = 46$) during a standard memory-guided saccade task (22). We measured activity during visual and saccade epochs and ranked each neuron using a visuomotor index (VMI) to quantify the respective response components. Our population of FEF neurons was biased toward visually responsive neurons, as expected (mean = 0.32, one-sample t test, $P < 10^{-3}$) (Fig. S3). Importantly, FEF neurons with significant CPs (21 of 46) showed a range of VMI values (Fig. S3*A*, filled bars), indicating that strength changes were not limited to motor-dominant neurons but found in visually dominant neurons as well. Finally, there were an equal number of visual- and saccade-related neurons with gCPs significantly greater than 0.5 ($n = 8$ for each) (Fig. S3*B*, filled circles). Hence, visual response strength changes were evenly distributed across visually responsive FEF neurons regardless of the presence of saccade-related activity.

Saccade-related activity can also influence visual responses and, in turn, CP values during fixation (12). Microsaccades, like standard saccades, have been shown to suppress visual activity (12, 23). For microsaccades to have explanatory power in our task, they needed to occur disproportionately more during short correct trials (compared with incorrect trials) and long incorrect trials (compared with correct trials), but this was not the case. For each monkey, we calculated the rate of microsaccades during the fixation epoch surrounding time interval presentation for all trials. Neither monkey showed significant differences in their rates of microsaccades that could account for our strength results. Monkey K showed no significant difference in short trials (rank-sum test, correct vs. incorrect; $P = 0.5$), but made significantly more microsaccades during correct long trials compared with incorrect long trials (rank-sum test, $P < 10^{-3}$). Monkey C showed significantly more microsaccades on incorrect short trials compared with correct short trials ($P = 0.02$), but no difference in long trials ($P = 0.23$).

SI Discussion

Complementary strength changes could also be related to systematic changes in attention. A priori, it seemed likely that strength changes would manifest as increased activity on correct trials regardless of the presented time interval. Enhanced activity, along with improvements in behavioral performance, is a hallmark of spatial attention (24). Although spatial attention likely played a role in our task (for example, by focusing neural resources on the location of the stimuli), attention by itself cannot account for our reported strength changes. Specifically, aberrations in spatial attention would not predict a relative increase in the size of second visual responses during incorrect short trials.

1. Mayo JP, Sommer MA (2008) Neuronal adaptation caused by sequential visual stimulation in the frontal eye field. *J Neurophysiol* 100(4):1923–1935.
2. Bruce CJ, Goldberg ME (1985) Primate frontal eye fields. I. Single neurons discharging before saccades. *J Neurophysiol* 53(3):603–635.
3. Bruce CJ, Goldberg ME, Bushnell MC, Stanton GB (1985) Primate frontal eye fields. II. Physiological and anatomical correlates of electrically evoked eye movements. *J Neurophysiol* 54(3):714–734.
4. Goldberg ME, Wurtz RH (1972) Activity of superior colliculus in behaving monkey. I. Visual receptive fields of single neurons. *J Neurophysiol* 35(4):542–559.
5. Lynch JC, Hoover JE, Strick PL (1994) Input to the primate frontal eye field from the substantia nigra, superior colliculus, and dentate nucleus demonstrated by transneuronal transport. *Exp Brain Res* 100(1):181–186.
6. Sommer MA, Wurtz RH (2004) What the brain stem tells the frontal cortex. I. Oculomotor signals sent from superior colliculus to frontal eye field via mediodorsal thalamus. *J Neurophysiol* 91(3):1381–1402.
7. May PJ (2006) The mammalian superior colliculus: Laminar structure and connections. *Prog Brain Res* 151:321–378.
8. Dow BM, Snyder AZ, Vautin RG, Bauer R (1981) Magnification factor and receptive field size in foveal striate cortex of the monkey. *Exp Brain Res* 44(2):213–228.
9. MacPherson JM, Aldridge JW (1979) A quantitative method of computer analysis of spike train data collected from behaving animals. *Brain Res* 175(1):183–187.
10. Sripati AP, Olson CR (2009) Representing the forest before the trees: A global advantage effect in monkey inferotemporal cortex. *J Neurosci* 29(24):7788–7796.
11. Efron B, Tibshirani R (1998) *An Introduction to the Bootstrap* (CRC, Boca Raton, FL), p xvi, 436 pp.
12. Herrington TM, et al. (2009) The effect of microsaccades on the correlation between neural activity and behavior in middle temporal, ventral intraparietal, and lateral intraparietal areas. *J Neurosci* 29(18):5793–5805.
13. Parker AJ, Newsome WT (1998) Sense and the single neuron: Probing the physiology of perception. *Annu Rev Neurosci* 21(1):227–277.
14. Green D, Swets J (1988) *Signal Detection Theory and Psychophysics* (Peninsula Publishers, Los Altos, CA), , Reprint Ed, pp xiii, 505 p.
15. Britten KH, Newsome WT, Shadlen MN, Celebrini S, Movshon JA (1996) A relationship between behavioral choice and the visual responses of neurons in macaque MT. *Vis Neurosci* 13(1):87–100.
16. Rolfs M, Kliegl R, Engbert R (2008) Toward a model of microsaccade generation: The case of microsaccadic inhibition. *J Vis* 8(11):5.1—5.23.
17. Hafed ZM, Goffart L, Krauzlis RJ (2009) A neural mechanism for microsaccade generation in the primate superior colliculus. *Science* 323(5916):940–943.
18. Engbert R, Kliegl R (2003) Microsaccades uncover the orientation of covert attention. *Vision Res* 43(9):1035–1045.
19. Maunsell JH, et al. (1999) Visual response latencies of magnocellular and parvocellular LGN neurons in macaque monkeys. *Vis Neurosci* 16(1):1–14.
20. Pouget P, Emeric EE, Stuphorn V, Reis K, Schall JD (2005) Chronometry of visual responses in frontal eye field, supplementary eye field, and anterior cingulate cortex. *J Neurophysiol* 94(3):2086–2092.
21. Mohler CW, Goldberg ME, Wurtz RH (1973) Visual receptive fields of frontal eye field neurons. *Brain Res* 61:385–389.
22. Hikosaka O, Wurtz RH (1983) Visual and oculomotor functions of monkey substantia nigra pars reticulata. III. Memory-contingent visual and saccade responses. *J Neurophysiol* 49(5):1268–1284.
23. Hafed ZM, Krauzlis RJ (2010) Microsaccadic suppression of visual bursts in the primate superior colliculus. *J Neurosci* 30(28):9542–9547.
24. Maunsell JH, Cook EP (2002) The role of attention in visual processing. *Philos Trans R Soc Lond B Biol Sci* 357(1424):1063–1072.

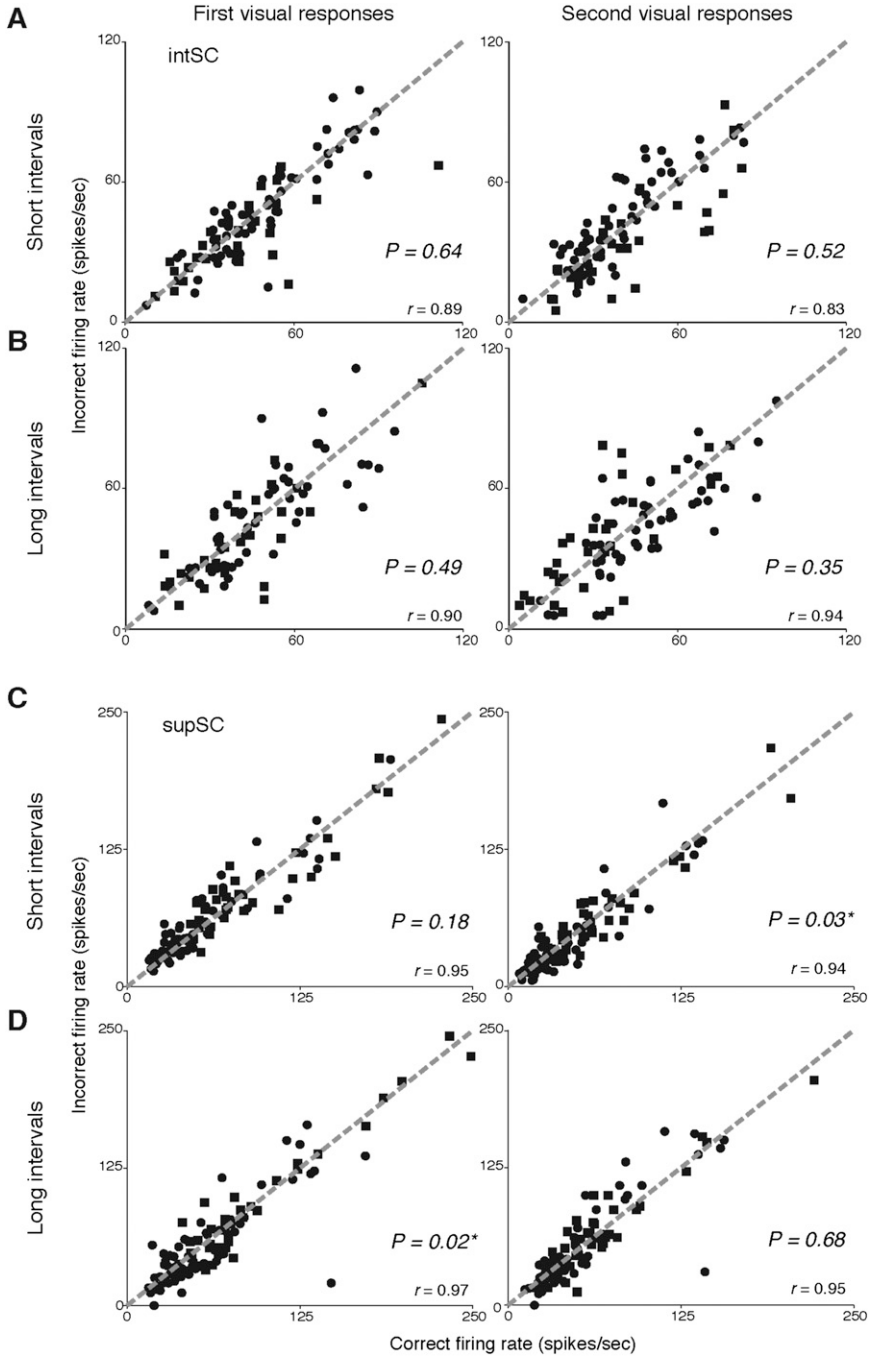

Fig. S1. Changes in intSC and supSC visual response strength as a function of behavioral performance. Same conventions as Fig. 3 *A* and *B*. Number of excluded outliers from each plot, for display purposes only: two from *A*, *Left*; three from *B*, *Left*; one from *C*, *Left*; two from *C*, *Right*; and one from *D*, *Left*. In the supSC (*C* and *D*), significant differences between correct and incorrect first visual responses (*D*, *Left*) were not a prediction of the strength hypothesis, and the direction of significant differences for second visual responses during short intervals (*C*, *Right*) ran counter to the prediction of the strength hypothesis.

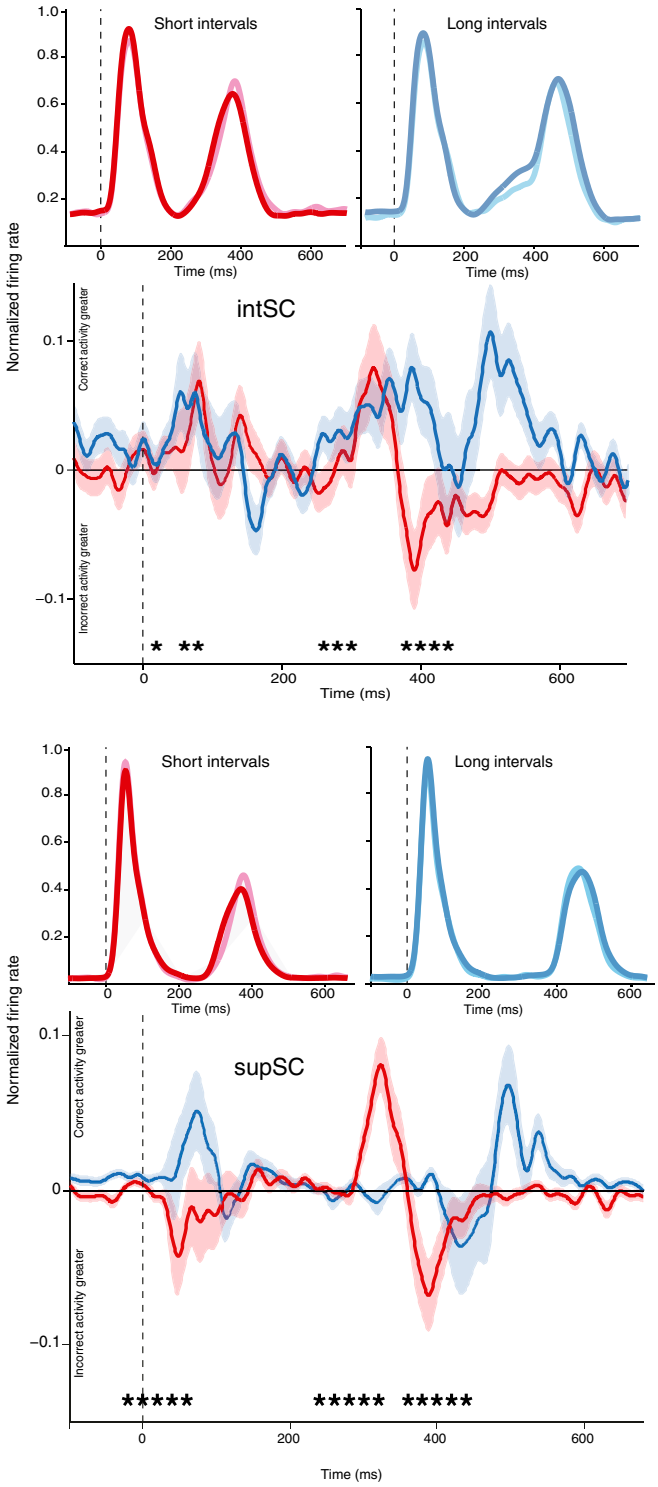

Fig. S2. Difference signals for the intSC (*Upper*) and supSC (*Lower*). Same conventions as Fig. 4*B*. Brief fluctuations were likely artifacts of the lower baseline firing rates in the SC, which led to apparent differences when the dynamics of responses (i.e., rise time and decay of visual responses) did not exactly match. Asterisks are centered on bins for which the "short" and "long" difference signals significantly diverged from each other ($P < 0.05$).

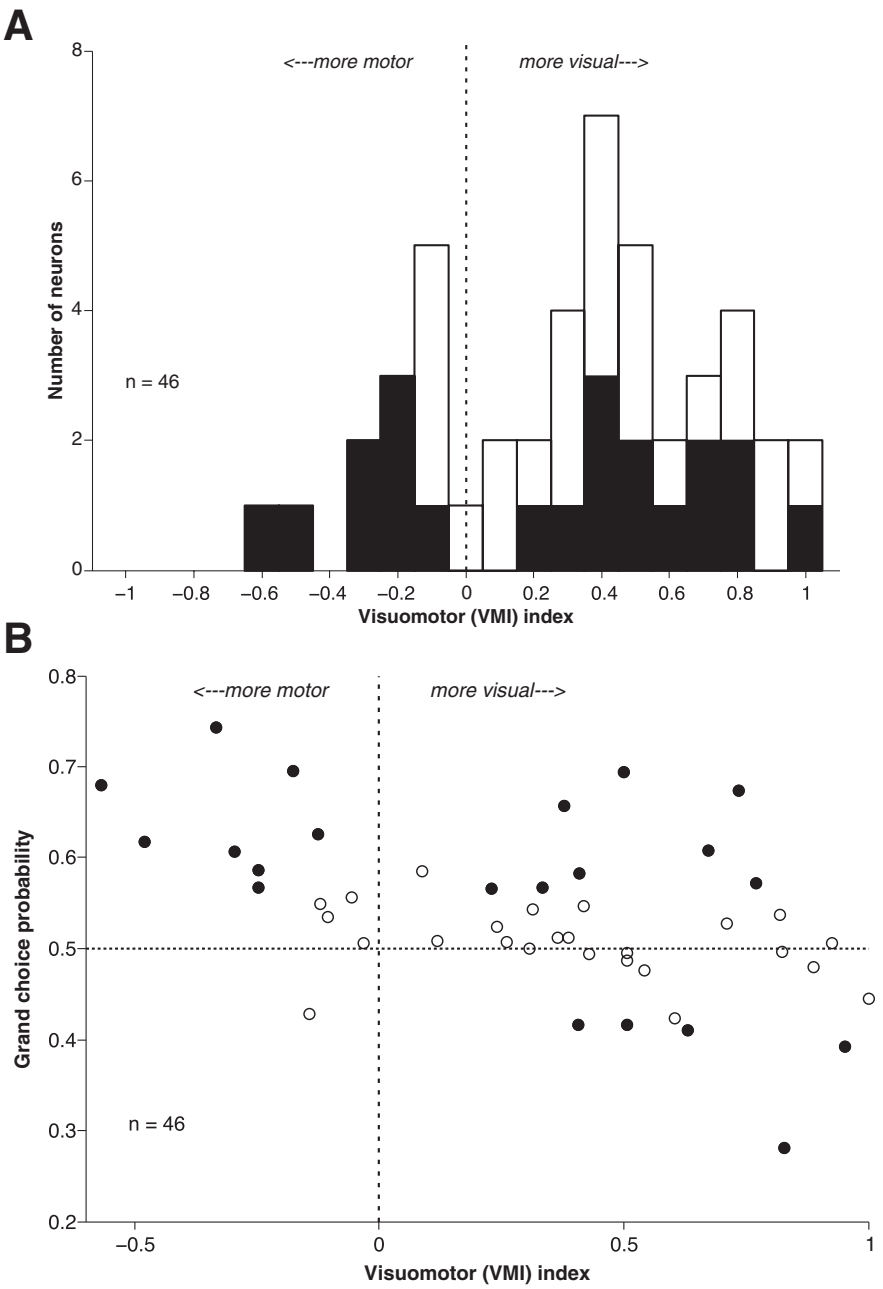

Fig. S3. Relationship between choice probability and visuomotor properties. (*A*) Visuomotor index (VMI = V − M/V + M) values of FEF neurons ($n = 46$). VMI of 1 indicates a purely visual neuron with zero saccade related activity and a VMI of −1 would indicate a purely saccadic neuron with no visual activity. All neurons had some visual activity and therefore the VMI was never below −0.6. Filled black bars indicate neurons with significant CPs ($n = 21$), which were located throughout the VMI range. (*B*) VMI of the same FEF neurons plotted as a function of their gCP values. Filled circles represent neurons with significant gCPs. High gCP values were found throughout the range of VMIs.

Table S1. Comparison of visual response latency metrics for FEF

Method	Mean	SD	Range: minimum	Range: maximum
SD2, SDF_5	66	16	44	113
SD2, SDF_10	65	16	41	113
Peak, SDF_5	87	20	55	150
Peak, SDF_10	88	21	57	146
MaxDiff	77	27	50*	150*
Poisson spike train	**64**	**19**	**29**	**118**
Poisson spontaneous rate	**73**	**33**	**3**	**152**
Poisson threshold	**64**	**22**	**8**	**120**
5% maximum	**58**	**19**	**20**	**97**

Top four white rows are latencies of first visual response onsets (correct trials only) for our FEF data ($n = 90$). Results in the bottom four boldface rows are from Pouget et al. (20). "SD2" refers to time that activity reaches two SDs above baseline activity. "Peak" refers to time that activity reaches its peak during visual response. SDF, spike density function, followed by the width of the Gaussian used (5 or 10). "MaxDiff" refers to a method that measures the time at which the visual response maximally differed from baseline activity, using a dynamic sliding window analysis (10). This method was not used during any other analysis and is shown only for reference. Latency methods in boldface are detailed elsewhere (20). Asterisks (*) indicate values that were limited by a fixed epoch size (50–150).

Table S2. Summary of first and second visual response latencies by metric

Visual response property	Onset				Peak				Offset				Duration (offset-onset)			
SDF width	5 ms		10 ms		5 ms		10 ms		5 ms		10 ms		5 ms		10 ms	
Which response?	First	Second	First	Second	First	Second	First	Second	First	Second	First	Second	First	Second	First	Second
FEF	66	58	65	55	87	82	88	82	128	112	143	123	62	54	78	68
intSC	54	46	49	39	77	70	80	70	123	107	131	112	69	61	82	73
supSC	39	35	34	31	54	57	55	56	107	96	119	107	68	61	85	76

Onsets, peaks, offsets, and durations of visual responses for two methods (5- or 10-ms kernel spike-density functions). Values (milliseconds) are means from correct trials. As discussed in the main text, second-response durations were always shorter than first-response durations (rightmost columns).

Table S3. FEF interresponse times do not conform to latency hypothesis

FEF		SDF 10 Short	SDF 10 Long	SDF 5 Short	SDF 5 Long
A	Onset-onset: SD2	Correct: 294 Incorrect: 296 $r^2 = 0.60$	Correct: 395 Incorrect: 397 $r^2 = 0.78$	Correct: 293 Incorrect: 293 $r^2 = 0.69$	Correct: 394 Incorrect: 396 $r^2 = 0.72$
B	Onset-onset: Peak	Correct: 292 Incorrect: 292 $r^2 = 0.46$	Correct: 394 Incorrect: 395 $r^2 = 0.56$	Correct: 293 Incorrect: 295 $r^2 = 0.46$	Correct: 395 Incorrect: 396 $r^2 = 0.44$
C	Onset-offset: SD2	Correct: 372 Incorrect: 373 $r^2 = 0.52$	Correct: 469 Incorrect: 466 $r^2 = 0.67$	Correct: 347 Incorrect: 349 $r^2 = 0.69$	Correct: 455 Incorrect: 451 $r^2 = 0.65$
D	Mean of shuffled	Correct: 287 Incorrect: 288 $r^2 = 0.61$	Correct: 392 Incorrect: 388 $r^2 = 0.71$	Correct: 287 Incorrect: 288 $r^2 = 0.58$	Correct: 391 Incorrect: 387 $r^2 = 0.68$
E	50% most reliable	Correct: 291 Incorrect: 289 $r^2 = 0.67$	Correct: 401 Incorrect: 394 $r^2 = 0.58$	Correct: 292 Incorrect: 291 $r^2 = 0.70$	Correct: 400 Incorrect: 395 $r^2 = 0.59$

Table of means (milliseconds) and correlation coefficients. Table cells are divided according to latency metric (rows) and width of spike density function (left two columns vs. right two columns). Because the latency hypothesis makes contrasting predictions for short and long time intervals, data were subdivided by interval group (short vs. long; columns within a SDF). Statistical significance of correct vs. incorrect latencies was determined using a signed-rank test ($P < 0.05$). Red shading indicates significance as predicted by the latency hypothesis. Gray shading indicates significance in the direction opposite to that predicted by the latency hypothesis. If the latency hypothesis is true then we should see two red boxes, horizontally side-by-side in the same row (for both short and long intervals). All correlation coefficients were significant, $P < 10^{-3}$.

Table S4. intSC and supSC interresponse times do not conform to latency hypothesis

intSC and supSC		Short	Long	Short	Long
intSC					
A	Onset-onset: SD2	Correct: 296 Incorrect: 299 $r^2 = 0.71$	Correct: 383 Incorrect: 385 $r^2 = 0.69$	Correct: 297 Incorrect: 299 $r^2 = 0.75$	Correct: 384 Incorrect: 385 $r^2 = 0.73$
B	Onset-onset: Peak	Correct: 299 Incorrect: 301 $r^2 = 0.66$	Correct: 379 Incorrect: 383 $r^2 = 0.43$	Correct: 301 Incorrect: 302 $r^2 = 0.52$	Correct: 381 Incorrect: 382 $r^2 = 0.41$
C	Onset-offset: SD2	Correct: 372 Incorrect: 367 $r^2 = 0.56$	Correct: 453 Incorrect: 452 $r^2 = 0.70$	Correct: 363 Incorrect: 354 $r^2 = 0.51$	Correct: 443 Incorrect: 438 $r^2 = 0.58$
D	Mean of shuffled	Correct: 298 Incorrect: 301 $r^2 = 0.73$	Correct: 380 Incorrect: 383 $r^2 = 0.63$	Correct: 300 Incorrect: 301 $r^2 = 0.69$	Correct: 382 Incorrect: 384 $r^2 = 0.66$
E	50% most reliable	Correct: 295 Incorrect: 295 $r^2 = 0.68$	Correct: 394 Incorrect: 396 $r^2 = 0.64$	Correct: 296 Incorrect: 296 $r^2 = 0.68$	Correct: 395 Incorrect: 395 $r^2 = 0.63$
supSC					
F	Onset-onset: SD2	Correct: 301 Incorrect: 305 $r^2 = 0.89$	Correct: 396 Incorrect: 395 $r^2 = 0.93$	Correct: 299 Incorrect: 304 $r^2 = 0.90$	Correct: 395 Incorrect: 395 $r^2 = 0.92$
G	Onset-onset: Peak	Correct: 307 Incorrect: 307 $r^2 = 0.85$	Correct: 397 Incorrect: 397 $r^2 = 0.92$	Correct: 310 Incorrect: 308 $r^2 = 0.72$	Correct: 398 Incorrect: 398 $r^2 = 0.83$
H	Onset-offset: SD2	Correct: 378 Incorrect: 375 $r^2 = 0.78$	Correct: 472 Incorrect: 465 $r^2 = 0.70$	Correct: 364 Incorrect: 354 $r^2 = 0.71$	Correct: 455 Incorrect: 456 $r^2 = 0.68$
I	Mean of shuffled	Correct: 306 Incorrect: 306 $r^2 = 0.94$	Correct: 397 Incorrect: 397 $r^2 = 0.96$	Correct: 307 Incorrect: 306 $r^2 = 0.93$	Correct: 398 Incorrect: 397 $r^2 = 0.96$
J	50% most reliable	Correct: 305 Incorrect: 302 $r^2 = 0.88$	Correct: 402 Incorrect: 402 $r^2 = 0.79$	Correct: 305 Incorrect: 304 $r^2 = 0.89$	Correct: 401 Incorrect: 400 $r^2 = 0.88$
		SDF 10		SDF 5	

Same conventions as Table S3. Red shading indicates significance as predicted by the latency hypothesis. Gray shading indicates significance in the direction opposite to that predicted by the latency hypothesis.